

# Design and Performance of a piezoelectric actuated precise rotary positioner

S. H. Chang and Y. C. Wang

<sup>2</sup>Department of Mechanical Engineering National Taiwan University, Taipei, Taiwan, ROC  
TEL: 886-2-2363-3863, FAX: 886-2-2363-1755  
e-mail: [shchang@ntu.edu.tw](mailto:shchang@ntu.edu.tw)

## Abstract

The need for nanometer resolution positioning technique draws significant attention for semi-conductor industry, biotechnology, and nanotechnology. This paper presents a design of friction-drive rotary stage driven by piezoelectric (PZT) actuator. This stage includes a multiplayer PZT actuator, Scott Russel mechanism, an actuation stage, a pre-load spring and an output shaft. The rotary positioning in this paper is accomplished by the stick-slip effect which a piezoelectric generated force is applied to produce an opposite angular momentums of the rotor to overcome the static friction and to achieve a relative motion. The optimum performance of the stage was achieved by adjusting the pre-load of a spring.

Finite element analysis and Taguchi optimization method were extensively conducted to analyze the displacement, stress and vibration behavior for optimum design.

Using the wire electro-discharge-machining (EDM), the rotary stage was fabricated and its performance was evaluated. The stage reaches the resolution of 0.13 rad and speed of 0.15 degrees per hour. The rotary positioner can be used in wafer fabrication and SEM for nano-manipulation.

**Keywords:** Piezoelectric actuated precise rotary positioner.

## 1. INTRODUCTION

Nowadays, every aspect of precision engineering is toward miniature and precision. The nanometer positioning systems are critical in semi-conductor industry, biotechnology, and nano-technology. As we are aware the characteristics of the PZT materials, the scopes of applications are widely increasing, such as PZT sensor, flight gyroscope, atomizer, printer head<sup>1</sup>, and nanometer positioning stage<sup>2</sup>.

In this study, a rotary stage actuated by a PZT ceramics was designed and tested. Taking advantage of PZT material such as small volume, fast response, low heat generation, high electric-mechanical coupling efficiency, high accuracy, and controllable feedback, the developed stick-slip positioning system has a high precision positioning accuracy with resolution of 0.13  $\mu$ rad. The traditional positioning system driven by stepping motors has rotary resolution of approximate 35  $\mu$ rad.

## 2. DESIGN

The stage in this study accomplished its rotation by use of the stick-slip effect. The stick-slip effect is a process that a force

is applied and induced an angular momentum of the rotor to overcome the static friction and to achieve a relative motion. In practical experiments, we operate PZT actuator moving in response to the input voltage signals in different kinds of waveforms. A rotor receives the driving force and transmits to the output shaft. When the input voltage drives the PZT actuator to move fast enough, both output shaft and actuator stage shall be subjected to an equal inertial force. If the inertial force is larger than the static friction force, the slip between the output shaft and the actuator stage could occur. Subsequently, the PZT's motion is slow such that the induced momentum and force would not exceed the maximum static friction and the relative motion ceases. In respond to the fast and slow motion of the PZT, the rotor will move and stay in sequence, and thus to complete the rotation. As the waveform of the input voltage is operated, the slip and stick motion can be sequentially controlled. The reversed rotary motion of the output shaft can be achieved in the reverse way.

Fig. 1 illustrates a Scott-Russell linkage<sup>8</sup>. Both points A and P in this linkage were constrained to allow motion of only one degree of freedom. While the point A moves along the X direction, the point P will move in the Y direction with the magnification ratio of  $Y_b / X_a$ . Therefore the linkage through expansion of the PZT material, the displacement at point P can be enlarged. Scott-Russell linkage is adapted in this design as the displacement magnification mechanism. The dotted line with notation OAMP in Fig. 2 shows the corresponding Scott-Russell linkage.

Fig. 2 and a photo in Fig. 3 showed the layout of PZT actuator stage fabricated by use of wire EDM to reach the required geometry and accuracy. The actuator stage was composed by a PZT, Scott-Russell linkage and rotary stage. A small displacement actuated by the PZT will be transmitted through these links to drive the rotary stage conducting reciprocating rotation. The rotary stage was supported by 4 leaf springs.

The purpose of this stage is to produce a motion of precise reciprocating rotation. When a voltage signal is applied to the PZT (1), due to piezoelectric effect, the PZT will expand along the positive Y direction. The displacement was magnified by the Scott-Russell linkage (2) and exerted a force in the X direction at point P of the linkage. The flexural hinges (3) and leaf springs (4) as shown in Fig. 2 were adapted to transmit the moment and guide the rotation precisely. The motion at the point P will move toward the positive X direction and the rotor receives the force and

rotates against its supports of four leaf springs. The rotation center will be at the symmetric point of the four leaf springs that shall be the geometric center of the stage. As the voltage signal vanished, the rotary stage would return to its initial position due to the elastic force of leaf springs and flexure hinges. By use of repeated voltage signals, the reciprocating rotation of the rotary stage can be achieved.

We used a torque output rod (9) to transmit the torque from the actuator stage (2) through rotor stage (4) and to the shaft as shown in Fig. 4.

The precision rotary positioning stage in this paper was achieved by extensive study of the friction characteristics to: (1) match the actuator-rotor inertial force with stick-slip effect. The ultra-precise displacement was due to high resolution of capability of PZT actuator.

Considering the harmonization and symmetry of the system, a slight wedge shape along the peripheral of the actuator stage and rotor stage was designed to avoid the angular momentum unbalance. An adjustable pre-load helix spring mechanism as shown in Fig. 4 was installed to find the appropriate compression force for the stick-slip effect. The whole rotary positioning mechanism is composed of inertial system, friction system, loading, guiding, and control system. Inertial system contains piezo-actuator, movable platform leaf spring, flexure hinge and torque output shaft. Friction system contains the friction interface between machined SKD-11 and SKD-9, pre-load spring and fixed-end of the spring offered by the upper cover. Loading contains upper cover and bottom case enabling the whole positioning system to work at vertical, horizontal and even upside down position. Guiding includes the ball bearing and thrust bearing. Control system includes function generator, power amplifier and AD/DA card.

### 3. ANALYSIS

#### 3.1 Finite element analysis

Considering the maximum stroke of PZT material is about  $17.4\mu\text{m}$ , the detailed configuration of a Scott-Russell mechanism was designed. Before fabricating, we setup a model using finite element software ANSYS to analyze rigidity, maximum rotation and working frequency of the actuator stage.

The actuator stage was modeled by using the 4-nodes element and Fig. 6 shows the finite element mesh. The static analysis results when the PZT exerts the force into Scott-Russell mechanism is shown in Fig. 7. The figure shows the displacement vector of the system under the input voltage of PZT at 100 V. The maximum rotation is  $155.96\mu\text{rad}$ . Compared with the maximum rotation measured by experimental results of  $104\mu\text{rad}$ , the efficiency of the rotary stage is approximately 67%. The difference may due to deformational strain energy of the system.

#### 3.2 Taguchi analysis

Taguchi analysis<sup>10</sup> is a statistic approach to solve the optimization problems. It practically is a very complicate

work to solve the problem with the eight parameters with 23 variances.

The developed statistic matrix allows the change of the variance and solves the required optimum target from the successive algorithm. From the Taguchi analysis of the eight parameters with 23 variances, two optimum objective functions were adapted in our study. In this case, "maximum rotation" and "minimum deviation of lateral displacement" were target function. The "rotation and the deviation" can be found from the analysis results of ANSYS model.

### 4. EXPERIMENTS

The precision rotary stage was fabricated by wire electro-discharge machining except that the PZT actuator was commercial product. Finished parts are shown in Fig. 3 and Fig. 8.

The setup of experiments is shown in Fig. 8. The characteristics of this rotary stage, such as angular rotation hysteresis of both the actuator stage and the rotary stage, were measured by Polytec laser interferometer with displacement resolution of 8 nm and bandwidth of 50 kHz. A photo reflected paper was pasted on the torque output rod in Fig. 3 to enhance the signal to noise ratio. The desired electric waveform was generated by WAVETEX model 9020 MHz synthesized function generator and amplified by the NF 4005 high-speed power amplifier. The signals were observed and recorded by using a Tektronix 2430A digital oscilloscope. The frequency response and impedance were both measured by using HP 35665A dynamic signal analyzer and HP 4194A impedance / gain-phase analyzer, respectively. A Kistler dual charge amplifier 9301A force transducer and Dytran 5850A piezo-hammer were used to measure the resonant frequency of this system. The tested stage was placed on the air-bearing supported optical table for vibration isolation.

The TOKIN made multi-layered PZT ( $5*5*20\text{ mm}$ ) containing 144 layers with layer thickness of  $108\mu\text{m}$ , density of  $800\text{ kg/m}^3$ , expands  $14.7\mu\text{m}$  under 150 V.

The first resonant frequency of multi-layered PZT ceramics measured by the HP impedance analyzer is 69 KHz as shown in Fig. 9 which is correspondent with the rated value of the TOKIN company.

We applied 20V to 80V voltage at frequency of 1 Hz to drive the PZT and measured its linear displacement of actuator stage. The results are shown in Fig. 10.

The hysteresis of the actuator stage shown in Fig. 11 was measured under -40 V to 40 V at 2 Hz, the output displacement is from  $-40.175\mu\text{m}$  to  $40.175\mu\text{m}$ .

The next measurements were to evaluate the rotor performance. Fig. 15 shows that both the impulse waveform of 30 V, 3 Hz and the rotational displacement output were recorded. The upper curve is the stepping motion of rotary stage (including the output shaft), 25 mV for each step and the corresponding displacement is  $2.5\mu\text{m}$ . The lower curve is the input impulse waveform of 3 Hz, 30 V.

The increment of each step corresponds to the rotation of  $2.5\mu\text{rad}$ . And under this output it will require 2,513,274

impulse voltages to make a 360-degree rotation. In other words, under a 50 V impulse at 10 Hz, we'll obtain the revolution as 0.15 degrees/hr.

Under the optimum working voltage (50V, 3Hz) of the stage, the experiments were made under various pre-load. The results are shown in Fig.14.

### 5. CONCLUSION

This paper describes the design, fabrication and experimental results of an ultra precision rotary stage. The positioning accuracy of the stage is 0.13μrad and the rotational speed is 13.61 degrees/hr. It normally operates at the upright mode as well as the upside down position. Both clockwise and counter-clockwise operations were achieved.

### Acknowledgement

Support under grant NSC-92-2212-E-002-012 from National Science Council is acknowledged.

### 6. REFERENCES

- [1]. B. Rogers, D. York, N. Whisman, M. Jones, K. Murray, J. D. Adams, T. Sulechek, and S. C. Minne, "Tapping mode atomic force microscopy in liquid with an insulated piezoelectric microactuator," *Rev. Sci. Instrum.*, vol. 73, pp. 3242, 2002.
- [2]. H. Isobe, T. Moriguchi and A. Kyusojin, "Development of Piezoelectric XYZ Positioning Device Using Impulsive Force," *Journal of the Japan Society for Precision Engineering*, vol. 62, no. 4, pp. 574-578, Apr. 1996.
- [3]. S. H. Chang and S. S. Li, "A high resolution long travel friction drive micropositioner with programmable step size," *The Review of Scientific Instruments*, vol. 70, no. 6, pp. 2776-2782, Jun., 1999.
- [4]. S. H. Chang and B. C. Du, "A precision Piezodriven Micropositioner Mechanism with Large Travel Range," *The Review of Scientific Instruments*, vol. 69, no. 4, 1998, pp. 1785-1791, 1998.
- [5]. S. H. Chang and C. K. Tseng and H. C. Chien, "An ultra-precision XY-z piezo-micropositioner, part II: experiment and performance," *IEEE Transactions, Ultrasonics, Ferroelectrics, and Frequency Control*, vol. 46, no. 4, pp. 906-912, July 1999.
- [6]. Jong-Youp Shim and Dae-Gab Gweon, "Piezo-driven metrological multi-axis nanopositioner," *Rev. Sci. Instrum.*, vol. 72, pp. 4183, 2001.
- [7]. Richard M. Seugling, Thomas LeBrun, Stuart T. Smith, and Lowell P. Howard, "A six-degree-of-freedom precision motion stage," *Rev. Sci. Instrum.*, vol. 73, pp. 2462, 2002.
- [8]. E. Ohmichi, S. Nagai, Y. Maeno, T. Ishiguro, H. Mizuno, and T. Nagamura, "Piezoelectrically driven rotator for use in high magnetic fields at low temperatures," *Rev. Sci. Instrum.*, vol. 72, pp. 1914, 2001.
- [9]. G. H. Martin and H. George, "Kinematics and Dynamics of Machines," pp. 52, McGraw-Hill Book Company, New York, 1982.
- [10]. P. J. Ross and J. Phillip, "Taguchi Techniques for Quality Engineering," McGraw-Hill Book Company, New York, 1989.
- [11]. Jun Hyung Kim, Soo Hyun Kim, and Yoon Keun Kwak, "Development of a piezoelectric actuator using a three-dimensional bridge-type hinge mechanism," *Rev. Sci. Instrum.*, vol. 74, pp. 2918, 2003.
- [12]. Richard M. Seugling<sup>9)</sup>, Thomas Lebrun, Stuart T. Smith and Lowell P. Howard, "A Six-degree-of-freedom Precision Motion Stage," *Rev. Sci. Instrum.*, vol. 73, pp. 2462, 2002.
- [13]. E. Ohmichi<sup>9)</sup>, Y. Maeno and T. Ishiguro, H. Mizuno and T. Nagamura, "Piezoelectrically Driven Rotator for Use in High Magnetic Fields at Low Temperatures," *Rev. Sci. Instrum.*, vol. 72, pp. 1914, 2001.

Table 1: Comparison of theoretical and experimental results

Item	Rotation (rad at 150V)
ANSYS analysis of actuator stage	155
Measured data of actuator stage	104
Measured data of slip-and-stick shaft	5.33

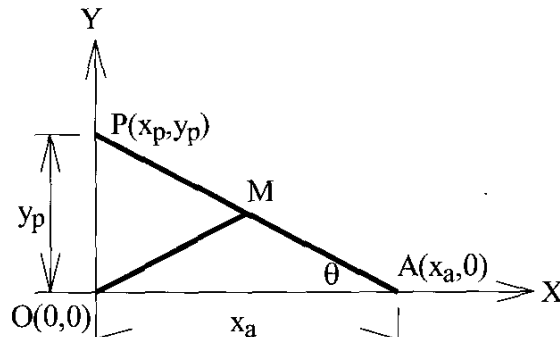


Fig. 1: A Scott-Russell linkage.

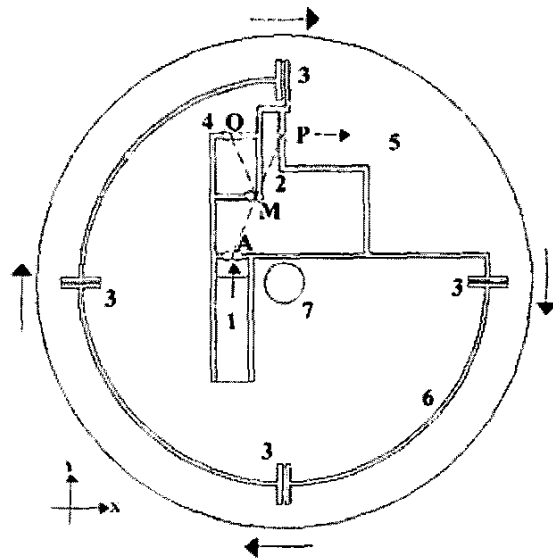


Fig. 2: Design of the actuator stage: (1) multi-layer PZT, (2) Scott-Russell linkage, (3) leaf spring (4 locations), (4) flexure hinge (4 locations), (5) rotor, (6) EDM clearance, (7) rotation center. Arrows indicate rotation of rotor.

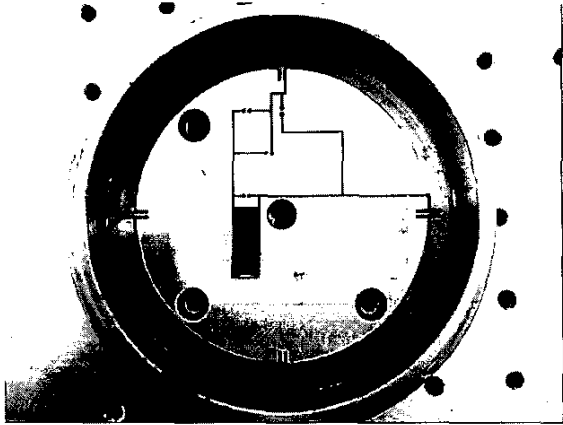


Fig. 3: A photo of the actuator stage sitting on optical table.

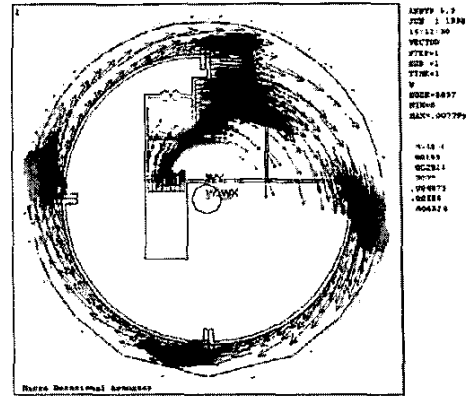


Fig. 7: Displacement vector plot of FEM simulation results.

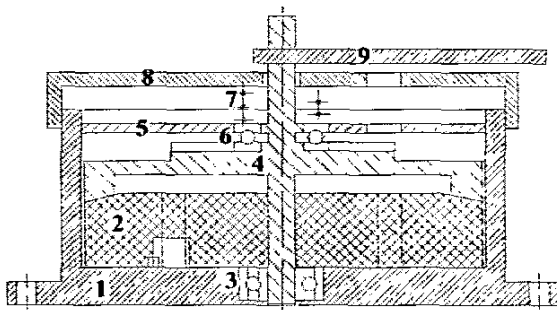


Fig. 4: Cross section of the stage assembly: (1) stationary case, (2) actuator stage (shown in Fig. 2), (3) ball bearing, (4) output shaft, (5) slip-and-stick loading disk, (6) thrust bearing, (7) spring for pre-load, (8) cover, (9) torque output rod.

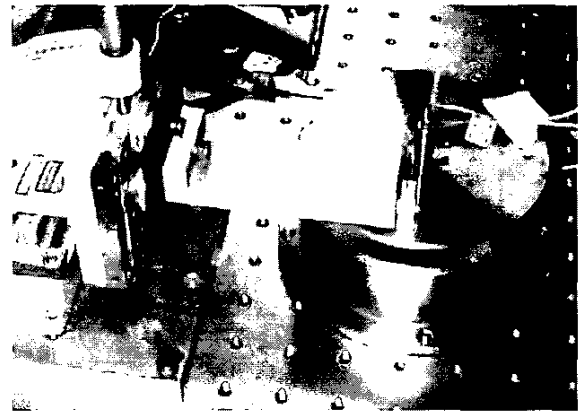


Fig. 8: A photograph of experiment set up.

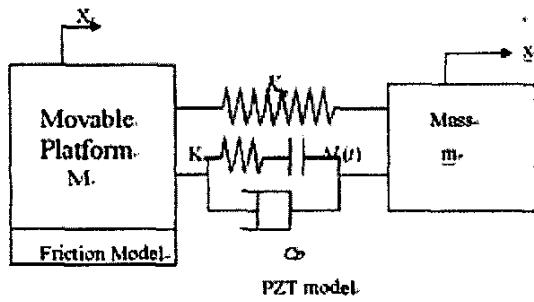
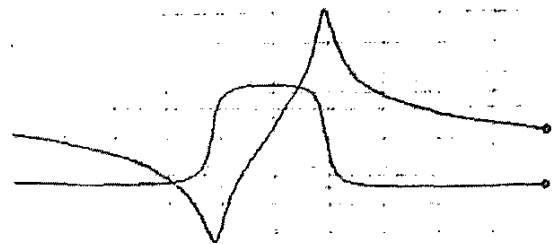


Fig. 5: Model of stick-slip drive positioning stage.

A:  Z	B: $\theta$	o MKR	100 000.000 Hz
A MAX 100.0	$\Omega$	MAG	2.38576 $\Omega$
B MAX 250.0	deg	PHASE	-86.9460 deg



A MIN 50.00	m $\Omega$		
E/DIV 50.00	deg		

Fig. 9: Measured impedance of piezoelectric actuator.

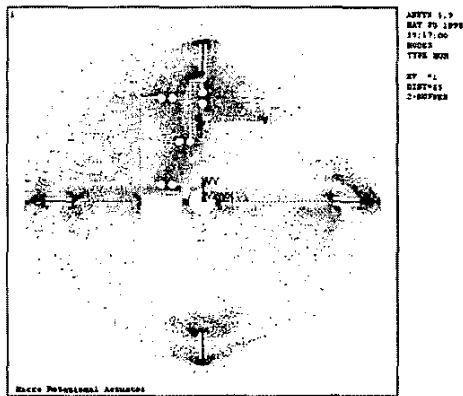


Fig. 6: A finite element modeling mesh.

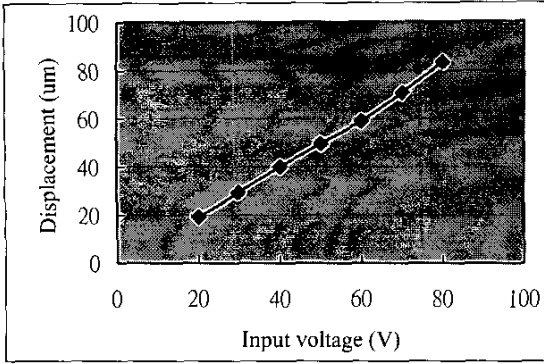


Fig. 10: Displacement of actuator stage operating at 1 Hz.

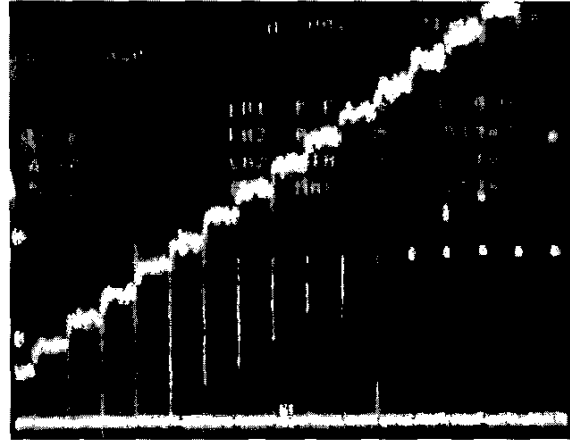


Fig. 13: Measured long travel stepping motion of rotary stage.

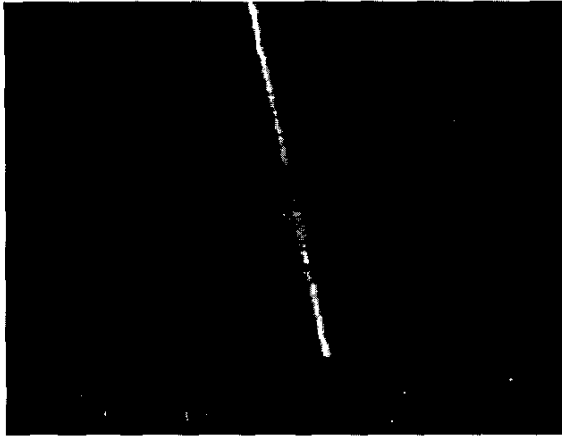


Fig. 11: Hysteresis curve of actuator stage, Horizontal axis: -40V to 40V, Vertical axis: -40.125 um to 40.125 um.

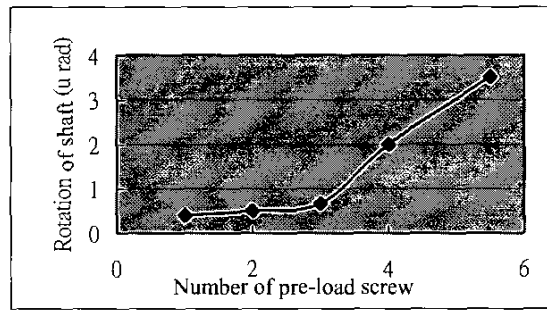


Fig. 14: Measured rotation of output shaft versus number of pre-load screw.

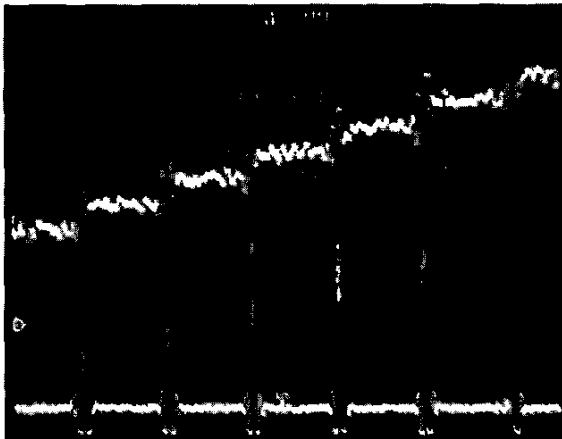


Fig. 12: Input impulse waveform (30V) (the lower curve) and the output displacement (the upper curve).